



# COMPARISON OF $\text{Ni}_{0.6}\text{Co}_{0.4}\text{Fe}_2\text{O}_4$ AND $\text{NiFe}_2\text{O}_4$ NANOPARTICLES FOR MAGNETIC CHARACTERISTICS, SYNTHESIZED USING CO-PRECIPITATION METHOD

Utari <sup>1\*</sup>, Yeni Herlina K. Dasi <sup>1,2</sup> and Budi Purnama<sup>1</sup>

<sup>1</sup>Department of Physics, Graduate School, Sebelas Maret University, Surakarta, Indonesia

<sup>2</sup>School of Engineering and Science, Institute Technology Dili, Rua ai -meti laran, Dili, Timur Leste

\*utarisby2013@staff.uns.ac.id

Received 06-02-2022, Revised 22-03-2022, Accepted 24-03-2022

Available Online 24-03-2022, Published Regularly April 2022

## ABSTRACT

Comparison of nickel  $\text{Ni}_{0.6}\text{Co}_{0.4}\text{Fe}_2\text{O}_4$  and  $\text{NiFe}_2\text{O}_4$  were studied. The co-precipitation method was performed for the whole sample. After annealing of  $600^\circ\text{C}$  for 4 hours, the nanoparticles samples evaluated their structural properties by using Fourier Transform Infra-Red (FTIR) and X-Ray Diffraction (XRD). The XRD pattern confirms that the whole samples have the crystalline structure of the face-centered cubic (fcc) inverse spinel. Furthermore, the lattice and crystallite size of  $\text{NiFe}_2\text{O}_4$  increased when added  $\text{Co}^{2+}$ . The FTIR spectrum showed two prominent absorption bands, i.e., at around  $k$  of  $358\text{ cm}^{-1}$  and  $588\text{ cm}^{-1}$ , where metals at tetrahedral and octahedral sites reflect intrinsic vibrations, respectively. Finally, the decrease of saturated magnetization  $M_s$  from  $22.2\text{ emu/g}$  and  $9.92\text{ emu/g}$  replacement of  $\text{Co}^{2+}$  cation with  $\text{Ni}^{2+}$ .

Keywords: cobalt ferrite; nickel ferrite; co-precipitation; magnetic characteristic.

## INTRODUCTION

Due to technological interests and attractive magnetic properties, the synthesis of spinel ferrite nanoparticles is becoming one of the most popular research fields. One essential spinel ferrite is cobalt ferrite which exhibits relatively high curie, high magnetostrictive coefficient, and appropriate saturation magnetization and electrical insulation <sup>[1-3]</sup>. These promising properties of cobalt ferrite allow it to be applied in various fields of high-density digital recording devices <sup>[4]</sup>, medical applications <sup>[5]</sup>, catalysts <sup>[6]</sup>, and others. In addition to its interesting application, changing the magnetic properties of cobalt ferrite can be done by adding doping to replace the ions in divalent or trivalent ions <sup>[7-8]</sup>. As in the research conducted by Kwang Joo Kim *et al.*, it was found that the  $\text{Ni}_{0.5}\text{Co}_{0.5}\text{Fe}_2\text{O}_4$  thin films made by the sol-gel process have spinel structure with lattice parameters that were slightly smaller by 0.1% compared to  $\text{CoFe}_2\text{O}_4$ . Where Co ions occupy the tetrahedral and octahedral sites, while Ni ions occupy most of the octahedral sites of the spinel lattice. Saturation magnetization, remanent magnetization, and Coercive field of  $\text{Ni}_{0.5}\text{Co}_{0.5}\text{Fe}_2\text{O}_4$  were reduced to 62%, 68%, and 29% <sup>[9]</sup>.

Nickel ferrite (NiFe<sub>2</sub>O<sub>4</sub>) nanoparticles are ferrite spinel magnetic nanoparticles with properties such as low melting point, high specific heating, expansion coefficient is large, saturation magnetic moment low magnetic transition temperature [10-11]. NiFe<sub>2</sub>O<sub>4</sub> nanoparticles are cubic ferromagnetic oxides with high permeability at high frequencies and high electrical resistance [12]. NiFe<sub>2</sub>O<sub>4</sub> nanoparticles exhibit ferromagnetic properties due to the anti-parallel magnetic moment pairing between the magnetic moments of Fe<sup>3+</sup> ions in the tetrahedral position, with the magnetic moments of Ni<sup>2+</sup> ions and Fe<sup>3+</sup> ions in the octahedral position. This ferrite system's remarkable electrical and magnetic properties depend on the properties of the ions, and the distribution between the tetrahedral and octahedral positions. NiFe<sub>2</sub>O<sub>4</sub> nanoparticles are soft ferrite material with characteristic ferromagnetic properties, low conductivity and low eddy current losses, high electrochemical stability, catalytic behavior and are widely available in nature [15]. NiFe<sub>2</sub>O<sub>4</sub> and CoFe<sub>2</sub>O<sub>4</sub> have an inverted spinel structure where (Ni<sup>2+</sup>Co<sup>2+</sup>) [Fe<sub>2</sub><sup>3+</sup>] O<sub>4</sub><sup>2-</sup> generally Fe<sup>3+</sup> are in octahedral and tetrahedral sites while Ni<sup>2+</sup> and Co<sup>2+</sup> are in octahedral sites [16].

There are two categories of 'bottom-up' and 'top-down' spinel ferrite synthesis methods. During 'bottom-up,' particles are formed when ions chemically combine. In the 'bottom-up,' there are many synthesis techniques: the co-precipitation technique. Co-precipitation is widely used because it is cost and time-efficient, environmentally friendly, and has high mass production [17-18]. This research will discuss the comparison of Ni<sub>0.6</sub>Co<sub>0.4</sub>Fe<sub>2</sub>O<sub>4</sub> and NiFe<sub>2</sub>O<sub>4</sub>. The Ni<sub>x</sub>Co<sub>1-x</sub>Fe<sub>2</sub>O<sub>4</sub> nanoparticle samples were synthesized using the co-precipitation method. Fourier transform infra-red (FTIR), x-ray diffractometer (XRD) were used to characterize the samples obtained, and magnetometry sample (VSM).

## METHODS

### Material

All the materials used in this report are of analytical grade and used without further purification Ni(NO<sub>3</sub>)<sub>2</sub>, Co(NO<sub>3</sub>)<sub>2</sub>.6H<sub>2</sub>O, Fe (NO<sub>3</sub>)<sub>3</sub>.9H<sub>2</sub>O, and Sodium hydroxide.

### Synthesis of Ni<sub>0.6</sub>Co<sub>0.4</sub>Fe<sub>2</sub>O<sub>4</sub> and NiFe<sub>2</sub>O<sub>4</sub>

The synthesis process is carried out through co-precipitation techniques, dissolving Ni(NO<sub>3</sub>)<sub>2</sub>, Co(NO<sub>3</sub>)<sub>2</sub>.6H<sub>2</sub>O, and Fe(NO<sub>3</sub>)<sub>3</sub>.9H<sub>2</sub>O for Ni<sub>0.6</sub>Co<sub>0.4</sub>Fe<sub>2</sub>O<sub>4</sub> nanoparticles. Whereas NiFe<sub>2</sub>O<sub>4</sub> nanoparticles, made by dissolving Ni(NO<sub>3</sub>)<sub>2</sub> and Fe(NO<sub>3</sub>)<sub>3</sub>.9H<sub>2</sub>O each with 200 ml of aqua-bides. Furthermore, it stirred using a magnetic stirrer at a speed of 300 rpm and heated at 350°C above the hot plate until it reached a temperature of 95°C. Then, the titration process is carried out by mixing 4.8 M NaOH into the solution (drop by drop). During the titration process, the solution temperature is maintained at 95°C. The synthesis solution is deposited for one night, then washed six times using ethanol and distilled water. Then, the precipitate was dried using an oven for 12 hours with a controlled temperature of 100°C and crushed to fine by mortar. Samples of Ni<sub>0.6</sub>Co<sub>0.4</sub>Fe<sub>2</sub>O<sub>4</sub> and NiFe<sub>2</sub>O<sub>4</sub> were in a *furnace* with 600°C aneling temperature variations and then crushed again for homogeneous results.

### Characterizations studies

The Ni<sub>0.6</sub>Co<sub>0.4</sub>Fe<sub>2</sub>O<sub>4</sub> and NiFe<sub>2</sub>O<sub>4</sub> samples that had been formed were then characterized. The structural properties of samples were characterized using *Cu-Kα*, radiation ( $\lambda = 1.54 \text{ \AA}$ ) for X-Ray Diffraction (XRD) D8 Advance Diffractometer,

Bruker, USA. The  $2\theta$  range was set at 25-70° with a step size of 0.02. The oxide bonds of the sample were characterized by Fourier Transforms Infrared (FTIR) spectroscopy (Shimadzu IR Prestige 21). The FTIR was recorded in the range 400- 4000 cm<sup>-1</sup>.

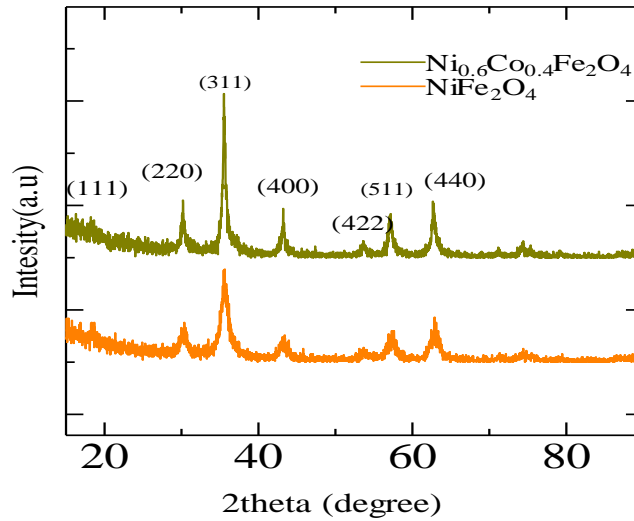


Figure 1. XRD pattern of NiFe<sub>2</sub>O<sub>4</sub> and Ni<sub>0.6</sub>Co<sub>0.4</sub>Fe<sub>2</sub>O<sub>4</sub> nanoparticles

## RESULTS AND DISCUSSIONS

### X-ray diffraction studies

X-ray diffraction pattern of NiFe<sub>2</sub>O<sub>4</sub> and Ni<sub>0.6</sub>Co<sub>0.4</sub>Fe<sub>2</sub>O<sub>4</sub> nanoparticles synthesized using the co-precipitation method at a temperature of 600°C (figure 1). Diffraction pattern based on ICDD nickel ferrite and all the peaks matches the characteristic reflection. Different peaks appear in the XRD pattern, namely  $2\theta = 18.5^\circ, 30.3^\circ, 35.6^\circ, 43.02^\circ, 53.9^\circ, 57.01^\circ$  and  $62.9^\circ$ . Formation of an inverted spinel structure with sharp peaks and planes observed, indicating Fd3m space group symmetry with single-phase formation (JCPDS Card No. 1-1121) [18]. The calculation of the crystallite  $D$ , based on Scherrer's equation

$$D = \frac{0.9\lambda}{\beta \cos\theta} \quad (1)$$

Where  $\lambda$  is the X-ray wavelength (1.540 Å),  $\beta$  is full width at half maximum (FWHM), and  $\theta$  is the diffraction angle. Table 1 gives the increase in crystal size ( $D$ ) in the presence of Cobalt ferrite, lattice parameter ( $a$ ) of all samples calculated individually using the formula

$$a = d\sqrt{h^2 + k^2 + l^2} \quad (2)$$

where  $d$  is the interplanar distance between two planes and ( $h, k, l$ ) are the Miller indices. The lattice parameter value increased with the addition of cobalt ferrite from 8.85 to 13.81. This is caused by the fact that Co<sup>2+</sup> has a larger ionic radius (0.74 Å) than Ni<sup>2+</sup> (0.69 Å), having a smaller ionic radius, which causes unit cell contraction. The X-ray densities ( $d_x$ ) was obtained from the equation

$$d_x = \frac{ZM}{NV} \quad (3)$$

where  $M$  is the molecular weight of the sample,  $N$  is Avogadro's number. The density of the sample with the addition of cobalt ferrite is smaller than that of nickel ferrite, and this is

related to the crystal size of the sample. Lattermost, the nickel ferrite strains decreased from  $8.85 \times 10^{-3}$  to  $13.81 \times 10^{-3}$  with the addition of cobalt ferrite.

**Table 1.** The calculation of crystalline parameters of Ni<sub>0.6</sub>Co<sub>0.4</sub>Fe<sub>2</sub>O<sub>4</sub> and NiFe<sub>2</sub>O<sub>4</sub> nanoparticles

Sample	Crystallite size <i>D</i> (nm)	Lattice parameter <i>a</i> (Å)	Density <i>d<sub>x</sub></i> (g/cm <sup>3</sup> )	Lattice strain $\epsilon$ ( $\times 10^{-3}$ )
NiFe <sub>2</sub> O <sub>4</sub>	8.85	8.352	5.344	12.80
Ni <sub>0.2</sub> Co <sub>0.8</sub> Fe <sub>2</sub> O <sub>4</sub>	13.81	8.377	5.298	8.23

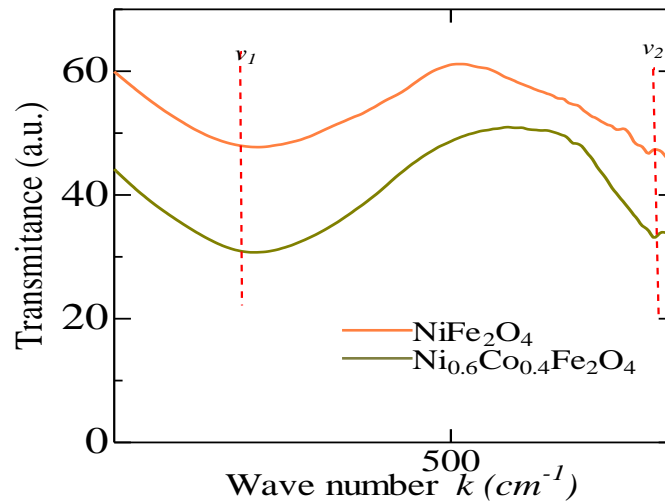


**Figure 2.** FTIR curves of NiFe<sub>2</sub>O<sub>4</sub> and Ni<sub>0.6</sub>Co<sub>0.4</sub>Fe<sub>2</sub>O<sub>4</sub> nanoparticles

### FTIR analysis

FTIR characterization for the analysis of the oxide bond of Ni<sub>0.6</sub>Co<sub>0.4</sub>Fe<sub>2</sub>O<sub>4</sub> and NiFe<sub>2</sub>O<sub>4</sub> samples (Figure 3) with a range of 4000 cm<sup>-1</sup> -350 cm<sup>-1</sup>. Characteristic of the observed curves for spinel ferrite, wave number  $\nu_1$  is in the range of 600 cm<sup>-1</sup>-500 cm<sup>-1</sup> and wavenumber  $\nu_2$  is around 450 cm<sup>-1</sup> -380 cm<sup>-1</sup>, which corresponds to the stretching of bonds between metal ions and oxygen at the tetrahedral and octahedral sites [17]. The absorption peaks observed for Ni<sub>0.6</sub>Co<sub>0.4</sub>Fe<sub>2</sub>O<sub>4</sub> and NiFe<sub>2</sub>O<sub>4</sub> were around 588.3cm<sup>-1</sup>-558.42 cm<sup>-1</sup> for the tetrahedral site and 376.14 cm<sup>-1</sup> – 358.78 cm<sup>-1</sup> for the octahedral site.

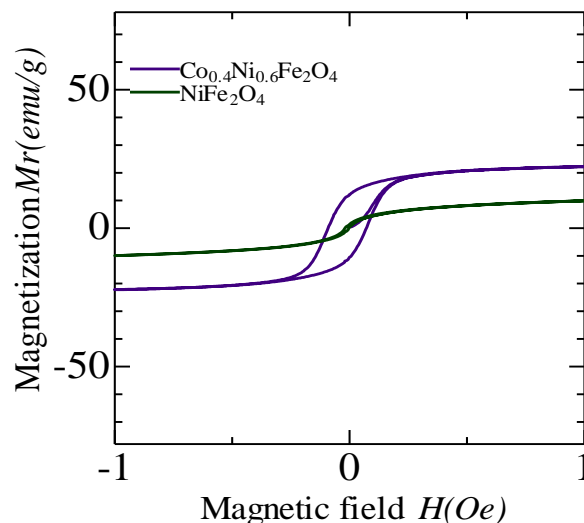


**Figure 3.** Hysteresis loop of NiFe<sub>2</sub>O<sub>4</sub> and Ni<sub>0.6</sub>Co<sub>0.4</sub>Fe<sub>2</sub>O<sub>4</sub> nanoparticles synthesized

## VSM analysis

The comparison of hysteresis loops between sample Ni<sub>0.6</sub>Co<sub>0.4</sub>Fe<sub>2</sub>O<sub>4</sub> and NiFe<sub>2</sub>O<sub>4</sub> has the same typical width and different saturation points (figure 3). Sample Ni<sub>0.6</sub>Co<sub>0.4</sub>Fe<sub>2</sub>O<sub>4</sub> has a larger hysteresis than NiFe<sub>2</sub>O<sub>4</sub>. Table 3 shows the presence of the enhancement in Ms, Hc, and Mr, of Ni<sub>0.6</sub>Co<sub>0.4</sub>Fe<sub>2</sub>O<sub>4</sub>, compared to NiFe<sub>2</sub>O<sub>4</sub>. The presence of cobalt ion increased the Mr and Ms of nickel ferrite from 1.96 emu/g to 12.33 emu/g and 9.92 emu/g to 22.2 emu/g.

**Table 2.** Coercive field (*H<sub>c</sub>*) and magnetization (*M<sub>s</sub>*) NiFe<sub>2</sub>O<sub>4</sub> and Ni<sub>0.6</sub>Co<sub>0.4</sub>Fe<sub>2</sub>O<sub>4</sub> nanoparticles

Sample	H <sub>c</sub> (Oe)	MS(emu/g)	Mr(emu/g)	Mr/Ms
NiFe <sub>2</sub> O <sub>4</sub>	123	9.92	1.96	0.379
Ni <sub>0.6</sub> Co <sub>0.4</sub> Fe <sub>2</sub> O <sub>4</sub>	793	22.2	12.33	0.511

## CONCLUSION

The suitable method obtained structural properties of NiFe<sub>2</sub>O<sub>4</sub> and Ni<sub>0.6</sub>Co<sub>0.4</sub>Fe<sub>2</sub>O<sub>4</sub> nanoparticles with an annealing temperature of 600°C for 4 hours. The XRD diffraction pattern of the two samples based on nickel ferrite ICDD, an inverted spinel structure with sharp peaks and planes, was observed, showing the symmetry of the Fd3m space group. Then, the crystal size and lattice parameters in nickel ferrite increase with the addition of cobalt ferrite because Co<sup>2+</sup> has a larger ionic radius than Ni<sup>2+</sup>, which has a smaller ionic radius. The FTIR spectrum showed two prominent absorption bands, namely around 588.3cm<sup>-1</sup>-558.42 cm<sup>-1</sup> for the tetrahedral site and 376.14 cm<sup>-1</sup> -358.78 cm<sup>-1</sup> for the octahedral site. The presence of cobalt ions in octahedral sites increases the *Mr* and *M<sub>s</sub>* of nickel ferrite because the magnetic moment of cobalt is much greater than that of nickel.

## ACKNOWLEDGMENTS

This research was funded by DIPA PNBP Universitas Sebelas Maret, Kementerian Riset, Teknologi, dan Pendidikan Tinggi, The Republic of Indonesia, contract No. 516/UN27.21/PP/2020.

## REFERENCES

- 1 Sedlacik, M., Pavlinek, V., Peer P., & Filip P. 2014. Tailoring the magnetic properties and magnetorheological behavior of spinel nanocrystalline cobalt ferrite by varying annealing temperature. *Dalton Trans.*, 43 (18), 6919–6924.
- 2 Carvalho, F.E., Lemos, L.V., Migliano, A.C.C., Machado J.P.B., & Pullar R.C. 2018. Structural and complex electromagnetic properties of cobalt ferrite (CoFe<sub>2</sub>O<sub>4</sub>) with an addition of niobium pentoxide. *Ceram. Int.*, 44, 915–921.
- 3 Lima, A.C., Peres, A.P.S., Araujo, J.H., Morales, M.A., Medeiros, S.N., Soares, J.M., Melo, D.M.A., & Carrico, A.S. 2015. The effect of Sr<sup>2+</sup> on the structure and magnetic properties of nanocrystalline cobalt ferrite. *Materials Letters*, 145, 56-58.
- 4 Routray, K.L., Sahoo, B., & Behera, D. 2018. Structural, dielectric and magnetic properties of nano sized CoFe<sub>2</sub>O<sub>4</sub> employing various synthesis techniques for high frequency and magneto recording devices: a comparative analysis. *Mater. Res. Express*. 5, 085016.
- 5 Srinivasan, S.Y., Paknikar, K.M., Bodas, D., & Gajbhiye, V. 2018. Applications of cobalt ferrite nanoparticles in biomedical nanotechnology. *Nanomedicine*, 13, 1221–1238.

- 6 Al-Anazi, A., Abdelraheem, W.H., Han, C., Nadagouda, M.N., Sygellou, L., Arfanis, M.K., Falaras, P., Sharma, V.K., & Dionysiou, D.D. 2018. Cobalt ferrite nanoparticles with controlled composition-peroxymonosulfate mediated degradation of 2-phenylbenzimidazole-5 sulfonic acid. *Appl. Catal. B Environ.*, 221, 266–279.
- 7 Anjum, S., Sehar, F., Bashir, F., Awan, M.S., & Mustafa, Z. 2015. Role of Bismuth in Cobalt Spinel Ferrite. *Materials Today: Proceedings*, 2(10), 5182-5189.
- 8 Lima, A.C., Peres, A.P.S., Araujo, J.H., Morales, M.A., Medeiros, S.N., Soares, J.M., Carrico, A.S. 2015. The Effect of Sr<sup>2+</sup> on the structure and magnetic properties of nanocrystalline cobalt ferrite. *Materials. Letter*, 145, 56–58.
- 9 Kim, K.J., Park, J., & Park, J.Y. 2020. Crystallographic and Magnetic Characteristics of Thin-film Ni<sub>0.5</sub>Co<sub>0.5</sub>Fe<sub>2</sub>O<sub>4</sub> Ferrimagnet. *Journal of Magnetism*, 25(2), 117-120.
- 10 Parishani, M., Cheragi, A., & Malekfar, R. 2015. Spectroscopy, Structural and Optical Investigations of NiFe<sub>2</sub>O<sub>4</sub> Ferrite. *International Journal of Optics and Photonics (IJOP)*, 9 (2), 73-78.
- 11 Bhise, R.B., Rathod, S.M., & Supekar, A.K. 2012. Synthesis and Characterization of nanocrystalline Ni-Co-Zn ferrite by Sol-gel Auto-Combustion Method. *International Journal of Scientific & Engineering Research*, 3 (12), 1-5.
- 12 Reddy, M.P., Madhuri, W., Sadhana, K., Kim, I. G., Hui, K.N., Hui, K.S., Kumar, K.V.S., & Reddy, R.R. 2014. Microwave sintering of Nickel Ferrite Nanoparticles Processed Via Sol-Gel Method. *J. Sol-Gel Sci. Technol.*, 70 (3), 400-404.
- 13 Safarik, I., Horska, K., Pospiskova, K., Maderova, Z., Safarikova, M. 2012. Microwave assisted synthesis of magnetically responsive composite materials. *IEEE Trans. Magn.*, 49, 213–218.
- 14 Lu Le, T., Dung Ngo, T., Tung Le, D., Thanh, C.T., Quy, O.K., Chuc, N.V., Maenosono, S., Thanh, N.T.K. 2015. Synthesis of magnetic cobalt ferrite nanoparticles with controlled morphology, monodispersity and composition: the influence of solvent, surfactant, reductant and synthetic conditions. *Nanoscale*, 7, 19596–19610.
- 15 Qasim, M., Asghar, K., Singh, B.R., Prathapani, S., Khan, W., Naqvi, A.H., Das, D. 2015. Magnetically recyclable Ni<sub>0.5</sub>Zn<sub>0.5</sub>Fe<sub>2</sub>O<sub>4</sub>/ Zn<sub>0.95</sub>Ni<sub>0.05</sub>O<sub>4</sub> nano-photocatalyst: structural, optical, magnetic and photocatalytic properties. *Spectrochim Acta A: Molecul Biomolecul Spect.*, 137, 1348–1356.
- 16 Stein, C.R., Bezerra, M.T.S., Holanda, G.H.A., Andre-Filho, J., Morais, P.C. 2018. Structural and magnetic properties of cobalt ferrite nanoparticles synthesized by coprecipitation at increasing temperatures. *AIP Adv.*, 8:056303.
- 17 Safi, R., Ghasemi, A., Shoja-Razavi, R., & Tavousi, M. 2015. The role of pH on particle size and magnetic consequence of cobalt ferrite. *Journal of Magnetism and Magnetic Materials*, 396, 288-294.